ASIAN JOURNAL OF CIVIL ENGINEERING (BUILDING AND HOUSING) VOL. 13, NO. 1 (2012)
PAGES 113-126

EXPERIMENTAL STUDY ON SHEAR STRENGTH OF HOLLOW CYLINDRICAL SPUN CAST CONCRETE ELEMENTS; LOCAL BEHAVIOUR

I. Völgyi* and Gy. Farkas
Department of Structural Engineering, BME, H-1111 Budapest, Műegyetem rkp. 3., Hungary

Received: 1 March 2011; **Accepted:** 7 August 2011

ABSTRACT

A parametric experimental study was carried out to analyse the local load carrying capacity and behaviour of hollow cylindrical RC specimens. This topic is part of a research program of shear-bending behaviour of hollow cylindrical members. Local load carrying capacity is important in the case of partially loaded members. The parameters of loading setup and specimens under research were: the loaded area, distance between support elements, angle of loading/support elements, wall thickness, length of specimen, transversal and longitudinal reinforcement.

Local failure modes of specimens were analysed through crack patterns and load-displacement diagrams. A mechanical model was created for calculation of the local behaviour of members. The model is able to calculate the resistance of hollow cylindrical members against partial loads. Analysis of the effect of local resistance utilization on shear-bending behaviour is possible using the proposed model.

Keywords: Spun-cast concrete, shear strength, parametric experimental study, hollow cylindrical cross section

Notation

A_s / A_{sw} Cross section area of longitudinal / helical reinforcement
F_a / F_b Ultimate frame / crump resistance of specimen
f_c / f_{ct} Mean value of cylinder compressive / tensile strength of concrete
f_{uw} Mean value of ultimate tensile strength of helical reinforcement
l Length of the specimen
s_w Spacing of the helical reinforcement
v Wall thickness of specimen
ρ_l Resultant reinforcement ratio
ρ_{lx} / ρ_{ly} Reinforcement ratio of the longitudinal / transversal reinforcement
ω Angle of center of the loading (and support) element

* E-mail address of the corresponding author: volgyi@vbt.bme.hu (I. Völgyi)

1. INTRODUCTION

Spun-cast concrete poles and piles are typical mass products in several countries. Spin-casting is an economical method for producing concrete elements with a long tradition. New fields of application are as columns of halls and buildings [2] or the structure of wind power plants. New requirements on these applications are ductility, shear strength, earthquake resistance. The topic of this research is the shear behaviour of hollow cylindrical members without a diaphragm. This paper examines the local behaviour of partially loaded members under shear-bending loading.

Researchers usually test compact cross sections or specimens with a plane grid. Formulas and theories for the calculation of shear strength of RC members are based on the test results of these experiment. A hollow cylindrical cross section has several specialties. It is also needed to prove whether the formulas in literature are safe and economical.

Shear resistance models used today are based on the shear truss analogy [3,4] or the modified compression field theory. Hollow cylindrical specimens do not have a grid parallel to the load. It is not easy to imagine which way are compressed struts able to work in this "curved grid". Do these specimens have another load carrying mode?

An important difference for the typical cross sections is the local behaviour. Spun cast concrete members are usually produced without diaphragms. In the case of partial loading, global behaviour of the member may be affected by the local stresses.

An experimental program was carried out to study the local and global behaviour of the members. The aim of the research was to recognize the local and global failure modes and behaviour and to analyse the crack pattern of different failure modes. A mechanical model for local behaviour is needed. The model should be able to calculate the local load carrying capacity in the case of the applied load type.

The information presented in this paper is the basis of a special shear resistance model for hollow cylindrical cross sections. The proposed model should be able to calculate the local behaviour utilization of member partially loaded by combined shear and bending. The results will help to analyse the relationship between the global shear-bending resistance and the utilization of the local resistance.

2. LOADING SETUP

Tests were carried out using a test machine of type WPM ZD600. The test setup is shown in Figure 1. Stiff steel elements were used in the load zone and in the support zones. Relative displacements of the upper to lower and of the left to right extreme fibers of the central cross section of the specimen were measured using inductance pick ups. Deformation in direction x vs y is called ovalization in this paper. Loading force was measured electronically too. Plastic bedding was placed between the specimen and the support/loading elements, see Figure 1.

The length and width of cracks were detected manually at each load step.

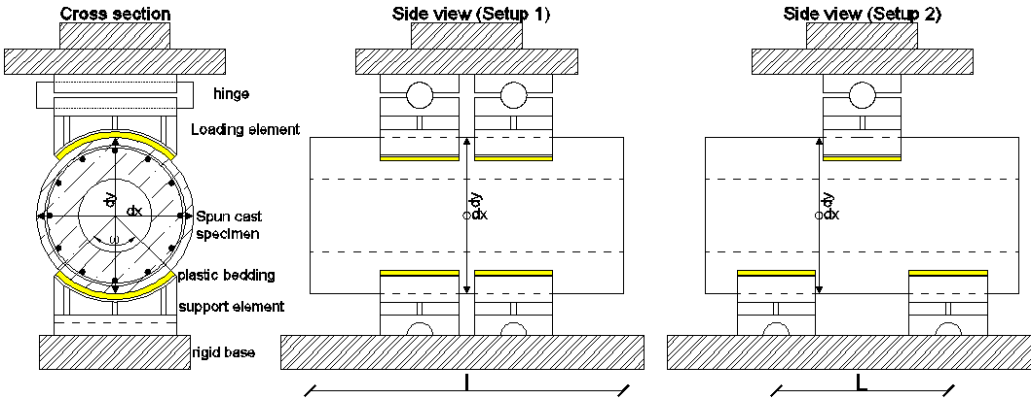

Figure 1. Loading setup

3. SPECIMENS, PARAMETERS

The outer diameter of all of the 24 specimens in the research was uniformly 300 mm.

One of the most important parameters of the local behaviour of this type of member is the wall thickness. The nominal wall thickness of the specimens was 55 or 90 mm.

The specimens were made using longitudinal and transversal reinforcement. Helical transversal reinforcement was used with a diameter of 5 mm. Some specimens were made without transversal reinforcement, others had a 150 or 75 mm pitch. The amount of transversal reinforcement affects the resistance of the cracked cross section. Each specimen was made using 12 pieces of longitudinal bar with a diameter of 10 or 14 mm. Longitudinal reinforcement may improve the effectiveness of the end zones of the specimen.

The lengths of the specimens varied too. The applied lengths were 330, 630, 930 or 1230mm. The length of the specimen is the other parameter of the load carrying of the end zones. The loading setup had parameters too. The angle of centre of support and of loading elements were chosen at 30°, 60° or 90°. The angle of centre assigns the type of the local behaviour. The number of loading surface element(s) and distance between support elements (L) were changed.

It is known that the structural behaviour of specimens depends on the type of loading. Both setups tested in research are shown in Figure 1. The first loading setup is able to show the specialties of clear local behaviour. The second loading setup is a model of the typical member under shear and bending. Interaction of the local and global behaviour can be shown through these specimens. The parameters of the specimens are summarized in Table 3.

4. MATERIAL PROPERTIES

Specimens are made of normal strength spun-cast concrete. The mixture was made of siliceous aggregate, high strength cement and had a low water/cement ratio. The data of the applied mixture are shown in Table 1. Preliminary tests were carried out to analyse the

mechanical properties of spun-cast concrete material. The results of this research are reported in reference [5] and [6]. The strength of the specimens was determined using an indirect method. The radial variation of rebound index was analysed on the end cross section and on the surface of the specimen. It was determined that specimens taking part in the research can be classed into compaction class IV. The strength of the extreme fibre of spun-cast concrete in compaction class IV is approximately 90% of the compressive strength of the vibrated cylinder specimen. The definition of compaction class can be found in [5]. For details on determining the compressive strength of spun-cast concrete material see reference [6]. The cylindrical compressive strength of the concrete material of the specimens is shown in Table 3.

Table 1: Mixture properties

Sand	**Silicous gravel**			**Crushed gravel**		**Cement type**	**Cement [kg]**	**Water [kg]**	**Superplasticizer**	**Fineness modulus**
0-4	2-8	4-8	8-16	0-5	5-12					
45%		25%	30%			CEM I 52,5 N	495	150	Stabiment FM 95E	6,00

The reinforcement of the specimens was with the usual reinforcement bars. The strength properties of the steel are summarized in Table 2.

Table 2: Mechanical properties of reinforcing steel

Diameter [mm]	**Yield strength [MPa]**	**Tensile strength [MPa]**
5	0	0
10	0	0
14	0	0

5. FAILURE MODES

Three different failure characterities were detected according to the combination of the parameters:

a. frame failure mode
b. crump
c. shear failure.

Analysis of the shear failure mode is the topic of the second part of this paper. Failure modes “a” and “b” are local failure modes. Both of them are analysed here.

5.1 Frame failure mode

This is the typical failure mode of specimens with a low angle of centre of loading element. The phenomenon is similar to the collapse of the RC pipes at standard quality control after EN

1916:2003. The differences of the phenomenon detected in the tests are caused by loading the specimen partially in the longitudinal direction and by the variation of the angle of centre of loading element. The crack pattern of short specimens is very similar to the pipes in literature [1]. Specimens are simple reinforced. Transversal reinforcement is installed, but only in the outer region of the wall. After cracking, no tensile resistance is available in the inner side of the wall. Upper and lower points of cross section (at 12 and 6 o'clock) do not have any bending moment resistance. Specimens without transversal reinforcement collapse at the moment of first cracking. Helical reinforcement in the middle height of the specimen works as longitudinal reinforcement of a rectangular axial wall section.

The crack pattern of the long specimens shows that the ovalization, as well as the effectiveness of cross sections far from the loading element is even lower. This means that the function of length to load bearing capacity is not linear.

The load-displacement relationship is similar to a cross section loaded by bending moment. The stiffness of the cross section is lower after the appearance of cracks. The ductility of behaviour mode is considerable. Ovalization diagram shows the change of behaviour. The dx/dy ratio is approximately equal to the Poisson's ratio in the first phase. The ratio is increasing up to the failure of the specimen. This increment is caused by the degradation of bending stiffness at 3 and 9 o'clock in the cross section.

Figure 2. Crack pattern of a short (EB1) and of a long specimen (EB8)

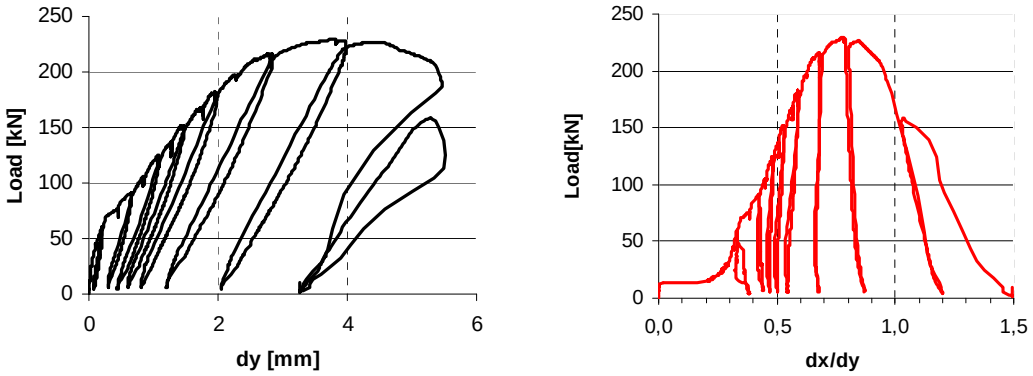

Figure 3. Typical diagrams of transversally reinforced specimens with frame failure mode

Table 3. Data of specimens and results of model

Name of specimen	Wall thickness [mm]	Diameter of lonitudinal reinforcement [mm]	Spiral spacing [mm]	Length of specimen [cm]	Number of loading elements	Number of support elements	Distance of support elements [cm]	Angle of center of loading elements [°]	Compaction class	Compressive strength of concrete [MPa]	Failure mode	Ultimate load [kN]	Resistance of behavior mode "a" [kN]	Resistance of behavior mode "b" [kN]	Local load carrying capacty of specimen [kN]	Calculated/measured ultimate load
EB1	55	10	75	63	2	2	18	60	IV	63,0	a	229,4	219,9	459,9	219,9	96%
EB2	55	10	150	63	2	2	18	60	IV	63,0	a	210,4	182,5	491,6	182,5	87%
EB3	55	10	75	63	2	2	18	90	IV	63,0	b	590,1	797,7	582,1	582,1	99%
EB4	55	14	75	93	2	2	18	90	IV	93,0	b	524,6	712,1	553,1	553,1	105%
EB5	55	10	150	123	1	2	88	90	IV	123,0	b	256,8	419,7	343,0		
EB6	90	10	75	93	2	2	18	30	IV	93,0	a	435,8	462,1	506,7	462,1	106%
EB7	90	14	75	93	2	2	18	30	IV	93,0	a	363,9	399,1	501,5	399,1	110%
EB8	55	10	75	93	2	2	18	60	IV	93,0	a	373,4	368,6	466,8	368,6	99%
EB9	55	10	150	33	2	2	18	30	IV	33,0	a	43,8	42,5	327,4	42,5	97%
EB10	55	10	75	93	2	2	18	90	IV	93,0	b	593,2	1038,1	558,6	558,6	94%
EB11	55	10	–	33	2	2	18	30	IV	33,0	a	16,9	17,5	246,8	17,5	104%
EB12	55	10	75	93	1	1	0	90	IV	93,0	a	469,0	1301,1	418,3	418,3	89%
EB13	55	14	150	93	2	2	18	90	IV	93,0	b	493,1	642,2	553,1	553,1	112%
EB14	55	10	75	93	2	2	18	30	IV	93,0	a	152,8	139,1	308,4	139,1	91%
EB15	55	10	75	93	1	1	0	90	IV	93,0	b	348,8	651,3	363,7	363,7	104%
EB16	55	10	75	63	4	4	18	30	IV	63,0	a	136,4	110,5	550,7	110,5	81%
EB17	55	10	75	63	2	2	18	30	IV	63,0	a	114,4	95,4	321,0	95,4	83%
EB18	90	10	75	33	2	2	18	30	IV	33,0	a	220,7	234,5	554,2	234,5	106%
EB19	55	10	75	93	1	2	65	90	IV	93,0	b-c	344,2	601,3	337,9	337,9	98%
EB20	55	10	–	33	1	2	18	90	IV	33,0	a	185,0	148,6	326,3	148,6	80%
EB21	55	10	150	123	1	2	85	90	IV	123,0	c	262,3	586,9	341,2		
EB22	55	10	75	93	1	2	45	90	IV	93,0	b	402,1	626,1	341,0	341,0	85%
EB23	55	10	75	93	1	2	55	90	IV	93,0	b-c	376,0	512,0	325,6	325,6	87%
EB24	55	10	75	93	1	2	35	90	IV	93,0	b	372,4	512,0	325,6	325,6	87%
															average:	95,5%
															deviation:	9,7%

5.2 Crump

The failure mode of the specimens of group “b” is the failure of concrete around the loading element. This is the typical failure mode of specimens with a large angle of centre of loading

element. The failure mode is similar to the punching of RC slabs in technical literature. The failure mode has also differences to punching. That is why a new expression is adopted.

Crump is a traditional expression of mining, it is the collapse of a tunnel. The difference to punching is caused by the curved shape of the cross section. The thickness of the "slab" varies along the critical perimeter. The first phase of the behaviour is similar to the behaviour of the type "a" specimens. First cracks appear at 6 and 12 o' clock at the inner extreme fiber of the wall. Additional cracks appear on the outer side at 3 and 9 o' clock later. The length and width of the cracks grow. The behaviour of the specimen is quasi bilinear in this phase.

After the first phase, a quasi brittle failure mode appears with a dislocation on the inner surface of the specimens around the loading (or support) element(s). The surface is similar to the punching surface of a slab around a column. The failure mode is brittle, plastic deformation is very small before the failure of the specimen. Figure 4 shows that cracks do not appear around the loading elements at lower load level. Critical cracks appear just before the failure of the specimen.

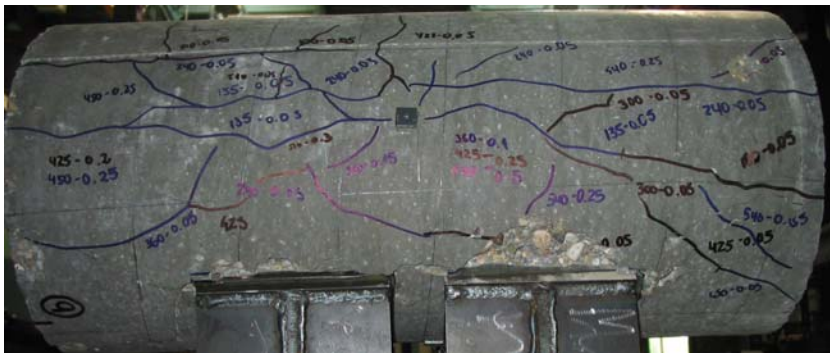

Figure 4. Crack pattern of specimen EB3 and dislocation around the support elements (bottom side view)

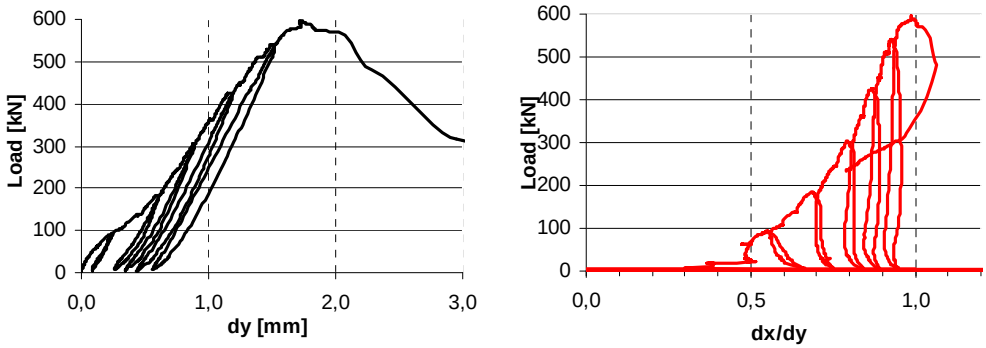

Figure 5. Typical diagrams of specimens with failure mode "b"

The load-ovalization diagram of the sample specimen (Figure 5) clearly shows the difference of the character of the punching failure mode to the frame failure mode (Figure 3). The first phase of the diagram is very similar to the frame failure mode. At the ultimate

load level, the direction of the curve changes. It shows the development of the new, brittle failure mode. In the case of crump, deformation in the y direction grows quickly. At the same time, x deformation does not increase significantly.

6. MECHANICAL MODEL

The local load carrying capacity of hollow circular RC specimens is a minimum of the resistance of the frame load carrying mode and of punching resistance. Two separate mechanical models are also created for approximation of the local resistance of the specimens. The mean values of the material properties and of the geometrical dimensions are applied in the models. The models are also able to approximate the mean value of the local resistance.

6.1 Frame failure mode

The frame failure mode is a bending failure of the rectangular longitudinal section at 3 and 9 o' clock due to eccentric compression. After cracking this curved frame opens at the upper and the lower point, see Figure 6. A hinge is also placed into the extreme fiber at 6 and 12 o' clock.

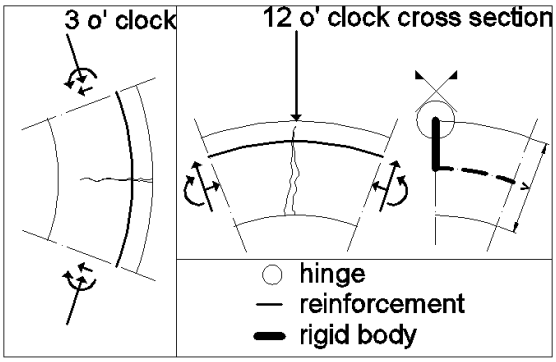

Figure 6. The frame at 3 and at 12 o' clock after crack appearance, and eccentric hinge at 12 o'clock

Stress distribution under the loading element (p) is not constant because of the ovalization of the specimen. The assumption of the model is a triangular distribution of stress under the rigid loading element, see Figure 7. The consequence of this stress distribution is a significantly higher horizontal joint load in the hinge at the same load level in the case of a large angle of centre at the loading element.

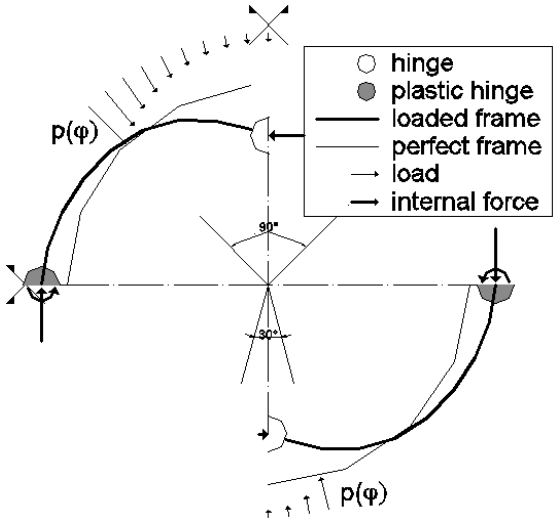

Figure 7.a Stress distribution under the loading element and horizontal force in the hinges in the case of angle of centre 30° and 90°

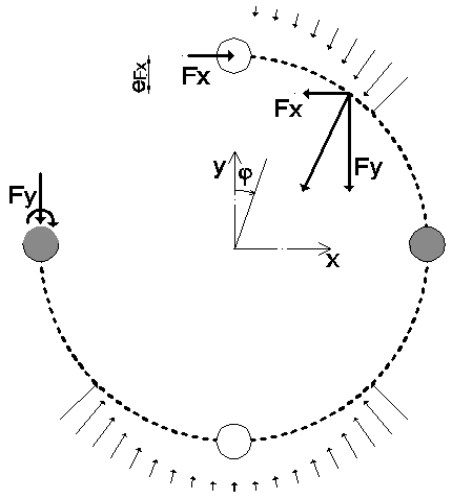

Figure 7.b Calculation of bending moment reduction in plastic hinge due to the eccentricity of horizontal forces

The eccentricity of the compression force in the plastic hinge can be calculated after equations 1-5.

$$F_x = \int_0^{0,5\cdot\omega} p(\varphi)\cdot \sin\varphi d\varphi \tag{1}$$

$$e_{Fx} = \frac{\int_0^{0,5\cdot\omega} p(\varphi)\cdot\sin\varphi\cdot r_{sz}(1-\cos\varphi)d\varphi}{F_x} \tag{2}$$

$$F_y = \int_0^{0,5\cdot\omega} p(\varphi)\cdot\cos\varphi d\varphi \tag{3}$$

$$M_{E3} = \int_0^{0,5\cdot\omega} p(\varphi)\cdot\cos\varphi\cdot\left(r_{sz} - \frac{v}{2} - r_{sz}\cdot\sin\varphi\right)d\varphi - F_x\cdot e_{Fx} \tag{4}$$

$$e_3 = \frac{M_{E3}}{F_y} \tag{5}$$

The effectiveness of the cross sections under the loading element is unity. This zone is expanded in a distance equal to the wall thickness because of the solid wall. It is assumed that effectiveness (ζ) builds down linearly to a distance equal to the diameter of the specimen, see Figure 8.

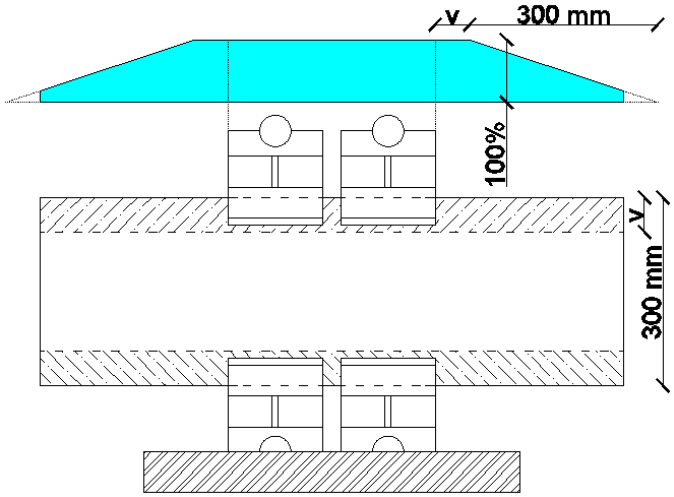

Figure 8. Explanation of effectiveness factor (ζ)

The width of the effective rectangular cross section (b^*) working at 3 and 9 o'clock also can be calculated after equation 6.

$$b^* = 2\cdot\int_0^{0,5\cdot l}\zeta(x)dx \tag{6}$$

The ultimate compression load (F_y) of the effective rectangular section at the calculated e_3 eccentricity can be found as half of the ultimate load of the frame behaviour mode. F_y is a half of the ultimate load of the specimen with failure mode type "a".

6.2 Crump

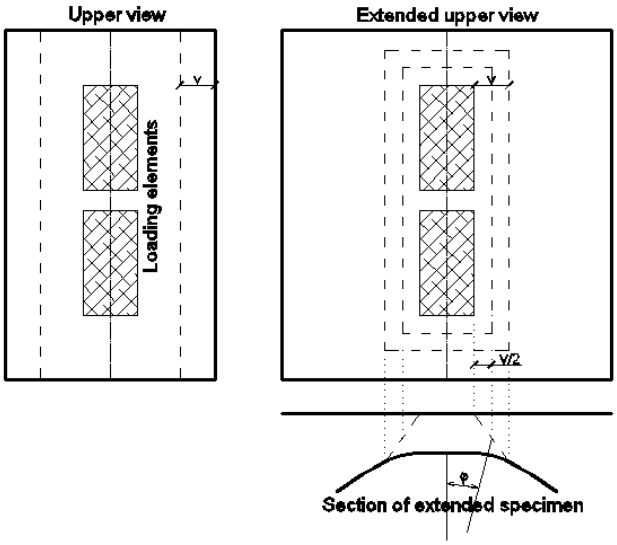

Figure 9. Explanation of projected specimen and control perimeter

The mechanical model of this behaviour mode is an equivalent slab projected onto a plane, explained in Figure 9. The thickness of the slab is a function of the angle from the direction of the load. The control perimeter to the loading elements distance is half of the wall thickness of the specimen. The effective thickness of the "slab" at the control perimeter is equal to the vertical projection of the wall thickness (equation 7). The shear stress along the control perimeter is taken to be uniformly distributed. The load transmitted by the loading elements is also taken to be concentric.

$$v^{*}(\varphi) = \frac{v}{\cos\varphi} \tag{7}$$

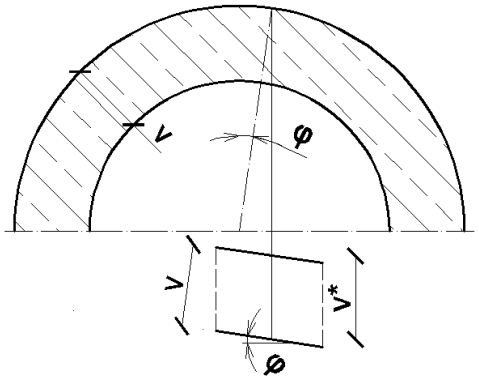

Figure 10. Explanation of effective wall thickness (v*)

No “punching shear reinforcement” is installed in the specimens. Both types of reinforcement applied in the specimens are orthogonal to the control surface. Both reinforcements are also compatible to the tension steel in the orthogonal direction of the usual plane slabs, see equation 8.

$$\rho_l = \sqrt{\rho_{lx} \cdot \rho_{ly}} \quad \rho_{lx} = \frac{\Sigma A_{sl}}{v \cdot K} \quad \rho_{ly} = \frac{\Sigma A_{sw}}{v \cdot s_w} \tag{8}$$

The proposed formula for calculation of crump resistance is equation 9.

$$F_b = \oint v^*(\varphi) \cdot f_{ct} \cdot \left(1 + \rho_l \cdot \frac{f_{uw}}{f_c}\right) \tag{9}$$

7. VERIFICATION OF PROPOSED MODEL

The proposed model was applied to the 24 specimens of the research. The results (see Table 3) were analysed in two ways.

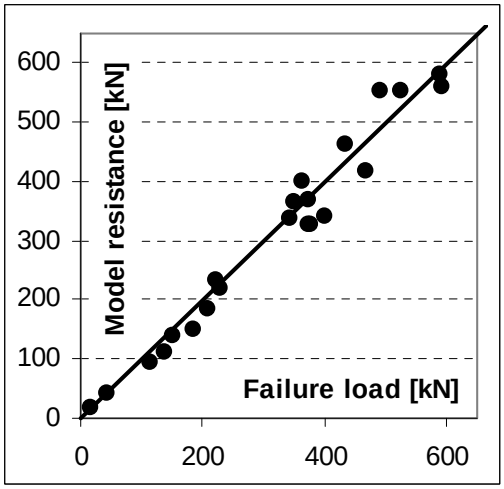

Figure 11. Calculated local load carrying capacity vs measured failure load diagram

The model should detect the type of the local failure mode. The identification of the failure mode by the model is correct at each specimen.

The second aspect is the calculated/measured resistance ratio. The results of the proposed model are reliable. The average of the calculated/measured resistance ratio is 95%. The standard variation of the ratio is under 10%. The proposed model is also able to approximate the mean local ultimate load of a hollow circular RC specimen.

8. APPLICATION OF PROPOSED MODEL TO REAL STRUCTURES

The applied load in the research is an idealization of real partial loads in the shear span of a member. The proposed model is able to be used for real loads of real structures after reduction of the real load to the idealized load tested in this research. The length and angle of centre of the loaded area has to be calculated. A very important parameter is the stiffness of the loading element. The stress distribution assumed in this paper is only valid in case of a rigid loading element. In the case of flexible loading element, it is proposed to ignore the horizontal component of $p(\varphi)$.

9. SUMMARY OF NEW SCIENTIFIC RESULTS

Conclusions for the specimens of the research are as follows.

- Local failure mode affects the shear-bending behaviour of hollow cylindrical RC members without diaphragms. The local load carrying capacity is the upper limit of the resistance of the member.
- Local failure modes of partially loaded hollow cylindrical RC members can be divided in two groups, named frame failure mode and crump.
- Typical crack patterns and characterities of load-displacement diagrams have been shown.
- A proposed model has been created to calculate the local load carrying capacity of members in the case of idealized loading tested in research.
- Analysis of the effect of local behaviour on shear-bending resistance is possible using the knowledge about the crack patterns and results of the local behaviour model.

Acknowledgement: The authors wish to express their gratitude to Lábatlani Vasbetonipari Zrt. for the research materials and for sponsoring the research. Thanks to the colleagues of the Structural Laboratory for their assistance in the laboratory work.

This work is connected to the scientific program of the "Development of quality-oriented and harmonized R+D+I strategy and functional model at BME" project. This project is supported by the New Széchenyi Plan (Project ID: TÁMOP-4.2.1/B-09/1/KMR-2010-0002).

REFERENCES

1. Bódi I, Erdődi L, Koris K. Parametric analyses of precast reinforced concrete pipes, *Proceedings of the 3rd Central European Congress of Concrete Engineering*, Visegrád, 2007, pp. 431-436.
2. Polónyi I, Walochnik V. Architektur und Tragwerk. Ernst & Sohn Berlin (2003) pp. 44-47, pp. 249-255,and pp. 256-260.
3. Turmo J, Ramos G, Aparacio A.C. Shear truss analogy for concrete members of solid and hollow circular cross section. *Engineering Structures* No. 2, (2009) 455–65.
4. Draskóczy A. Main Directions of Standardization in Shear Design, *Concrete Structures,*

Annual Technical Journal of the Hungarian Group of Fib, **4**(2003) 59-66.
5. Völgyi I, Farkas Gy. Determination of strength of spun-cast concrete elements, *Fifth International PhD DLA Symposium in Engineering* 2009, pp. 70-71.
6. Völgyi I, Farkas GY, Nehme SG. Concrete Strength Tendency in the Wall of Cylindrical Spun-Cast Concrete Elements, *Periodica Polytechnica Civil Engineering* No. 1, **54**(2010)23-30.